

## Encapsulation of Olive Leaf Extract in $\beta$ -Cyclodextrin

IOANNIS MOURTZINOS,<sup>†</sup> FOTINI SALTA,<sup>†</sup> KONSTANTINA YANNAKOPOULOU,<sup>‡</sup>  
ANTONIA CHIOU,<sup>†</sup> AND VAIOS T. KARATHANOS<sup>\*,†</sup>

Laboratory of Chemistry-Biochemistry-Physical Chemistry of Foods, Department of Nutrition & Dietetics, Harokopio University, El. Venizelou 70., Kallithea, 176 71 Athens, Greece, and Institute of Physical Chemistry, National Center for Scientific Research 'Demokritos', Aghia Paraskevi, 15310 Athens, Greece

Olive leaf extract, rich in oleuropein, formed an inclusion complex with  $\beta$ -cyclodextrin ( $\beta$ -CD) upon mixing of the components in aqueous media and subsequent freeze-drying. Inclusion complex formation was confirmed by differential scanning calorimetry (DSC). DSC thermograms indicated that the endothermic peaks of both the olive leaf extract and the physical mixture of olive leaf extract with  $\beta$ -CD, attributed to the melting of crystals of the extract, were absent in DSC thermogram of inclusion complex. Moreover, DSC studies under oxidative conditions indicated that the complex of olive leaf extract with  $\beta$ -CD was protected against oxidation, since it remained intact at temperatures where the free olive leaf extract was oxidized. Phase solubility studies afforded  $A_L$  type diagrams, 1:1 complex stoichiometry, a moderate binding constant ( $\sim 300 \text{ M}^{-1}$ ), and an increase of the aqueous solubility by  $\sim 50\%$ . The formation of the inclusion complex was also confirmed by nuclear magnetic resonance (NMR) studies of  $\beta$ -CD solutions in the presence of both pure oleuropein and olive leaf extract. The NMR data have established the formation of a 1:1 complex with  $\beta$ -CD that involves deep insertion of the dihydroxyphenethyl moiety inside the cavity from its secondary side.

**KEYWORDS:** Phase solubility; nuclear magnetic resonance; differential scanning calorimetry; oleuropein; olive leaves; inclusion complex; natural antioxidants

### INTRODUCTION

Encapsulation of active compounds has been extensively used during the past decades in the cosmetics and drugs industry in order to provide protection against oxidation, increased solubility, and increased activity when consumed orally. In the food industry encapsulation is being used for many purposes such as flavors carrier and to impart of protection against evaporation of volatile compounds, reaction, or migration in a food; thus, it may be used for preparation of several fortified foods and functional foods (1, 2). During the recent years nutraceuticals are considered as health-promoting ingredients of food; thus, encapsulation can provide them with necessary protection against oxidation (3).

Cyclodextrins (CDs), formed by the enzymatic modification of starch (4), are cyclic glucose oligomers having six, seven, or eight glucose units linked by 1,4- $\alpha$ -glucosidic bonds, termed as  $\alpha$ -,  $\beta$ -, and  $\gamma$ -cyclodextrin, respectively. The hollow molecular shape allows them to form inclusion complexes with a wide variety of organic compounds, which enter partly or entirely into their relatively hydrophobic cavity, simultaneously expelling the few high-energy water molecules from the interior. The

cavity size of the CDs offers selectivity for the complexation of guest molecules (5). The physical, chemical, and biological properties of molecules, which are encapsulated by CDs, may be thus drastically modified (6). Encapsulation may lead to dissolution rate enhancement, increased membrane permeability, and bioavailability of low-solubility nutraceuticals. CDs may also act as flavor carriers and provide protection against oxidation, light-induced decompositions, and heat-induced changes. Moreover, CDs may prolong the shelf life of food products and mask or reduce undesired taste and odor (7).

The leaves of the olive tree *Olea europaea*, a member of the family Oleaceae, have been widely used in folk medicine in regions around Mediterranean Sea and the islands therein (8, 9). The main constituents of olive leaves are secoiridoids like oleuropein, ligostroside, dimethyloleuropein, and oleoside (10). Olive leaves also contain flavonoids (apigenin, kaempferol, luteolin) as well as phenolic compounds (caffeic acid, tyrosol, hydroxytyrosol).

Oleuropein, the main constituent of olive leaf extract, is a complex phenol present in large quantities in olive tree leaves and in low quantities in olive oil (11) and is responsible for the bitter taste and pungent aroma of olive oil. In vitro studies have demonstrated that oleuropein acts as an antitumor compound (12), inhibits platelet-activating factor activity (13), enhances nitric oxide production by mouse macrophages (14), and decreases inflammatory mediator production (15). It has also

\* To whom correspondence should be addressed (telephone ++30-210-9549224; fax ++30-210-9577050; e-mail vkarath@hua.gr).

<sup>†</sup> Harokopio University.

<sup>‡</sup> National Center for Scientific Research 'Demokritos'.

been found to inhibit in vitro the mycoplasma (human pathogenic bacteria) (16). Studies in rats indicate that oleuropein prevents oxidative myocardial injury (17). Recent studies demonstrated that oleuropein might be a modulator of metabolism (18), while the anti-ischemic, antioxidative, and hypolipidemic effects of oleuropein in anesthetized rabbits were most recently evaluated (19).

Oleuropein can be hydrolyzed to hydroxytyrosol, elenolic acid, oleuropein aglycone, and glucose (17). Hydrolysis can be achieved either chemically (20) or enzymically (21). For the enzymic hydrolysis a hyperthermophilic  $\beta$ -glycosidase immobilized on chitosan has been used, and high amounts of hydroxytyrosol were produced (22).

The molecular encapsulation of olive leaf extract into  $\beta$ -cyclodextrin could result in increased aqueous solubility or increased partitioning in the oil/water system (23), improved protection against oxidation during storage, and, possibly, a better bioavailability. In addition to the above, the encapsulated olive leaf extract could result in a product that can be used readily as a food ingredient, in a better way than olive leaf extract alone, due to its solid form and its possible increased stability against heat and oxidation. The interaction of oleuropein with  $\beta$ -cyclodextrin has only been described previously using light scattering techniques (24). In the present work the inclusion of the constituents of olive leaf extract was studied extensively with methods such as differential scanning calorimetry (DSC) and nuclear magnetic resonance (NMR) spectroscopy. NMR is widely used to obtain detailed information about the structure of an inclusion complex in aqueous solution (25, 26), while DSC is used to confirm the formation of a complex in the solid state. The disappearance of thermal events of guest molecules, such as the endothermic peak assigned to melting, when examined as CD complexes is generally considered as a proof of inclusion (27, 28). Moreover, DSC can be used under oxidative conditions to study the oxidation of a compound (29). Olive leaf extract solubility in the presence of  $\beta$ -CD was also determined by a phase solubility study.

## MATERIALS AND METHODS

**Samples, Standards, and Solvents.** Olive tree (*Olea europaea*) leaves were collected from the Thermopylae region (Greece), belonged to the 'Kalamon' cultivar, and were kept at 4 °C until analysis. Oleuropein and hydroxytyrosol were obtained from Extrasynthèse (Genay, France);  $\beta$ -CD, quercetin, bis(trimethylsilyl)trifluoroacetamide (BSTFA), and 3-(4-hydroxyphenyl)-1-propanol were purchased from Aldrich (Steinheim, Germany). Tyrosol, protocatechuic acid, and caffeic acid were obtained from Fluka (Steinheim, Germany). 4-Hydroxybenzoic acid, *p*-hydroxyphenylacetic acid, *p*-coumaric acid, and ferulic acid were obtained from Sigma (Steinheim, Germany). All reagents were used as received. Methanol, hexane, acetone, acetonitrile, chloroform, and ethyl acetate of analytical grade and methanol of HPLC grade were obtained from Merck (Darmstadt, Germany). Deionized water was used for the preparation of the complexes and the phase solubility experiments.

**Preparation of Olive Leaf Extract.** Olive leaf extract was prepared according to the procedure described by Gariboldi (9) with slight modifications. Briefly, leaves (100 g) were macerated and extracted in methanol (500 mL) for 3 days, by a batch process, in the dark, at room temperature. Subsequently, the extract was filtered, and the solvent was evaporated under reduced pressure. The residue was redissolved in 100 mL of acetone-water (1:1) and washed with hexane (4  $\times$  25 mL) and chloroform (4  $\times$  25 mL), followed by ethyl acetate extraction (4  $\times$  25 mL). The ethyl acetate extracts were combined, the solvent was evaporated under vacuum, and the residue was dissolved in methanol (5 mL). The extract was kept at 4 °C, in hermetically sealed glass containers after application of inert gas, until further analysis and use.

**High-Performance Liquid Chromatography of Olive Leaf Extract.** An HPLC system (Agilent Technologies, model 1050, Waldbronn, Germany) combined with quaternary pump, autosampler, diode array detector (HP-1050), fluorescence detector (HP-1046A), and data analysis software was used. A binary solvent system consisting of water acidified with phosphoric acid (pH 3) and methanol was used, with gradient elution on a Nucleosil C18 100-5 (125 mm  $\times$  4.6 mm) column (MZ, Mainz, Germany) at flow rate 1 mL/min as follows: initially 10% methanol to 18% methanol within 10 min; 28% methanol in 10 min; isocratic for 5 min; 31% methanol within 17.5 min; 34% methanol within 2.5 min; isocratic for 10 min; 40% methanol within 5 min; isocratic for 2.5 min; 70% methanol in 7.5 min; 80% methanol in 10 min; and finally to the initial conditions within 10 min. A 10 min post-run for the system equilibration was used. UV detection (280 and 254 nm) plus fluorescence detection ( $\lambda_{\text{ex}} = 275 \text{ nm}$ ,  $\lambda_{\text{em}} = 360 \text{ nm}$ ) was applied. Olive leaf extract prepared as described in the former paragraph was diluted 1:50, and 10  $\mu\text{L}$  was injected. External standard quantification was performed based on a series of five different standard oleuropein concentrations (9.0–144  $\mu\text{g/mL}$ ).

**Gas Chromatography/Mass Spectrometry of Olive Leaf Extract.** An Agilent (Wallborn, Germany) HP series GC 6890N coupled with a HP 5973 MS detector (EI, 70 eV), split-splitless injector and an HP 7683 autosampler were used. Prior to GC analysis, olive leaf extract was diluted 1:100 v/v in methanol, and 0.05 mL was mixed with internal standard 3-(4-hydroxyphenyl)-1-propanol (20  $\mu\text{L}$ , 19.2  $\mu\text{g/mL}$ ), evaporated to dryness under nitrogen, and derivatized by the addition of 250  $\mu\text{L}$  of BSTFA at 70 °C for 20 min. An aliquot (1  $\mu\text{L}$ ) of derivatized sample was injected into the gas chromatograph at a split ratio 1:20. Analysis of sample was achieved using an HP-5 MS capillary column (5% phenyl-95% methylsiloxane, 30 m  $\times$  0.25 mm  $\times$  250  $\mu\text{m}$ ). The chromatographic conditions applied are described elsewhere (30). A selective ion monitoring (SIM) GC/MS method was applied for detection of 25 target polyphenolic compounds. Detection of polyphenols was based on the  $+0.05RT$  presence of target and qualifier ions of the standard polyphenols at the predetermined ratios. Target and qualifier ions for the 25 polyphenolic compounds and the internal standard are described elsewhere (30). Linearity was obtained for all target compounds detected in samples in the range of quantitation limit and up to 20 times higher concentrations of each compound.

**Preparation of the Inclusion Complex.** The olive leaf extract (0.025 g) was dispersed in 10 mL aqueous solution of  $\beta$ -CD (9 mM) at a mole ratio 1:2 (calculations were based on the molecular weight of oleuropein, since this compound was the main constituent of the olive leaf extract) and left under stirring for 72 h at room temperature. Subsequently, the suspension was frozen at  $-40 \text{ }^\circ\text{C}$  for 24 h and then lyophilized in a freeze-dryer (Telstar, Cryodos, Terrassa, Spain).

**Preparation of the Physical Mixture.** Olive leaf extract (0.025 g) was admixed with  $\beta$ -CD (0.103 g) at the same mole ratio as the one used for the preparation of the inclusion complex using mortar and pestle for 5 min to obtain an homogeneous blend.

**Phase Solubility Studies.** Phase solubility studies were carried out according to the method described by Higuchi and Connors (31). An excess amount of olive leaf extract was mixed in an aqueous solution containing increasing amounts of  $\beta$ -CD (0–0.015 M) at 25, 35, and 45 °C using a laboratory shaker. The amount of olive leaf extract in solution, after equilibrating for 3 days, was determined spectrophotometrically at 254 nm. Prior to measurement, the samples were filtered through a 0.45  $\mu\text{m}$  PTFE filter. The experiments were carried out in triplicate at each temperature. Stability constant calculations were based on the molecular weight of oleuropein, since this compound was the main constituent of the olive leaf extract (90.2%) as revealed by HPLC and GC analysis (Table 1).

The stability constants,  $K_c$ , were calculated from the phase solubility diagram according to the Higuchi–Connors equation (eq 1):

$$K_c = \frac{\text{slope}}{\text{intercept} \cdot (1 - \text{slope})} \quad (1)$$

**Study of Complex Formation by DSC.** A Perkin-Elmer DSC instrument (DSC-6, Boston, MA) was used. Temperature calibration was carried out using indium metal. In order to identify differences in DSC curves, four different types of samples were tested:  $\beta$ -CD, olive

**Table 1.** Polyphenolic Species Identified and Quantified in the Olive Leaf Extract

polyphenol	amount (mg/kg olive leaf)
oleuropein	1680 ± 103.67
hydroxytyrosol	34.1 ± 1.12
quercetin	52.2 ± 5.40
ferulic acid	11.2 ± 1.55
caffeic acid	19.5 ± 1.27
<i>p</i> -hydroxyphenylacetic acid	7.1 ± 2.27
<i>p</i> -coumaric acid	15.5 ± 0.63
tyrosol	13.8 ± 1.29
<i>p</i> -hydroxybenzoic acid	9.0 ± 1.49
protocatechuic acid	11.9 ± 0.67
vanilethanediol	8.5 ± 0.17

leaf extract, physical mixture, and inclusion complex. The scan rate was 10 °C/min between 70 and 230 °C under a nitrogen environment. Samples were weighed at ±0.01 mg accuracy and placed in 40 μL closed aluminum pans. Duplicate determinations were carried out for each sample.

**Study of the Decomposition of Olive Leaf Extract and Its Inclusion Complex by DSC.** DSC studies were performed to study the stability against thermal oxidation of the samples. Samples of olive leaf extract, ~2 mg or a quantity of the complex of olive leaf extract with β-CD containing the same amount of olive leaf extract, were placed in aluminum pans with one hole in their lid. The specimens were heated from room temperature to 120 °C in an oxygen atmosphere at a heating rate of 90 °C/min. The oxygen atmosphere was provided by connecting the DSC instrument to an oxygen container that provides the gas. Samples remained at 120 °C for 1 min to ensure a homogeneous temperature distribution within the sample and then heated up to 400 °C at a heating rate of 10 °C/min.

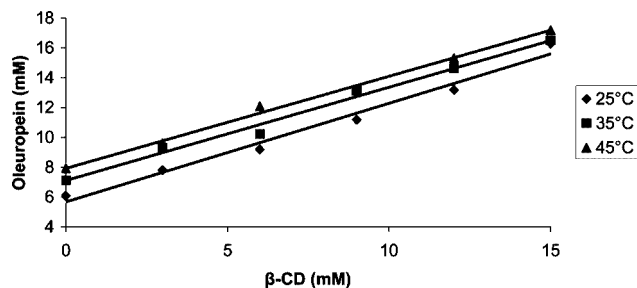
**NMR.** <sup>1</sup>H NMR spectra were acquired on a Bruker Avance DRX spectrometer at 500 MHz in unbuffered D<sub>2</sub>O solutions at 298 °C. 2D ROESY spectra were acquired at 298 K with presaturation of the residual water resonance and a mixing (spin-lock) time of 350 ms at a field of ~2 kHz, using the TPPI method.

**Statistical Analysis.** All DSC experiments were duplicated. Analyses concerning the olive leaf extract polyphenol content were triplicated. The results presented are the average of the obtained values. Data handling was carried out using Microsoft Excel.

## RESULTS AND DISCUSSION

The polyphenol content of the olive leaf extract was determined by HPLC and GC/MS analysis. Results were expressed in terms of olive leaves content and are presented in **Table 1**. Identification of oleuropein by HPLC analysis was based on the retention time and ultraviolet spectrum of standard oleuropein. Quantification of oleuropein was based on the absorbance at 254 nm. Other polyphenols were also detected and quantified by GC/MS analysis. In this latter case identification of chromatographic peaks was achieved by comparing the retention times and ratios of three fragment ions of each polyphenol with those of reference compounds (SIM method). Internal standard quantification was performed based on a series of nine standard mixtures of the polyphenolic compounds containing the same quantity of internal standard as that of samples. On the basis of the results of GC/MS analysis, the olive leaf extract was found to contain hydroxytyrosol, quercetin, ferulic acid, caffeic acid, (*p*-hydroxyphenyl)acetic acid, *p*-coumaric acid, tyrosol, *p*-hydroxybenzoic acid, protocatechuic acid, and vanilethanediol. Among the polyphenols identified, oleuropein comprised 90.2% of the total polyphenol content. This extract was used in all studies that followed.

Phase solubility studies were carried out at three temperatures to calculate the stability constants,  $K_c$ , and the thermodynamic values for the formation of complexes of olive leaf extract with

**Figure 1.** Phase solubility study of olive leaf extract with β-CD in water at 25, 35, and 45 °C (calculations were based on oleuropein's molecular weight).**Table 2.** Phase Solubility Study Parameters and Stability Constants,  $K_c$ , of Olive Leaf Extract/β-CD Complexes at Different Temperatures (25, 35, and 45 °C)

temperature (°C)	intercept	slope	<i>R</i>	$K_c$ (M <sup>-1</sup> )
25	0.0057	0.659	0.9821	339
35	0.0071	0.626	0.9893	236
45	0.0079	0.616	0.9945	203

**Table 3.** Thermodynamic Values for Complex Formation of Olive Leaf Extract with β-CD Based on Phase Solubility Studies

thermodynamic parameter	value
Δ <i>H</i> (kJ mol <sup>-1</sup> )	-20.2
Δ <i>S</i> (J mol <sup>-1</sup> K <sup>-1</sup> )	-19.7
Δ <i>G</i> <sub>25</sub> (kJ mol <sup>-1</sup> )	-14.3

β-CD. The phase solubility diagrams of the complexes at different temperatures (25, 35, and 45 °C) are presented in **Figure 1**. Results are expressed in terms of oleuropein concentration since this compound is the major component of the extract. Oleuropein solubility was increased more than 150%, as this constituent was encapsulated in β-CD (**Figure 1**). As shown in **Figure 1**, the plots are linear ( $R^2 > 0.982$ , **Table 1**) and the slope is <1, at each of the temperatures studied; therefore, all can be considered as A<sub>L</sub>-type diagrams (30), indicating 1:1 binding. The corresponding stability constants,  $K_c$ , of the complex formation as calculated using eq 1 are given in **Table 2**. Information presented in **Table 2** is in accordance with the fact that the solubility of olive leaf extract in water increased with temperature (intercept of lines) as well as the total concentration of this composite in aqueous media containing β-CD increased at higher temperatures. The values of  $K_c$  decreased with increasing temperature, indicating an exothermic binding process (31, 32).

The phase solubility data also provided the thermodynamic parameters involved in the complex formation. The integrated form of the van't Hoff equation (eq 2) under constant pressure permits the calculation of the values of enthalpy and entropy changes, based on the variations of the stability constants with temperature (32):

$$\ln k_c = -\frac{\Delta H}{RT} + \frac{\Delta S}{R} \quad (2)$$

The van't Hoff plot for the complex of olive leaf extract/β-CD was a linear function of  $K_c$  and the inverse of the absolute temperature (1/*T*). The thermodynamic parameters (Δ*H*, Δ*S*) calculated are presented in **Table 3**. The negative values of enthalpy changes indicated that the interaction processes of olive leaf extract with β-CD are exothermic. The enthalpy change (Δ*H*) was -20.2 kJ mol<sup>-1</sup>, which is relatively small, typical of



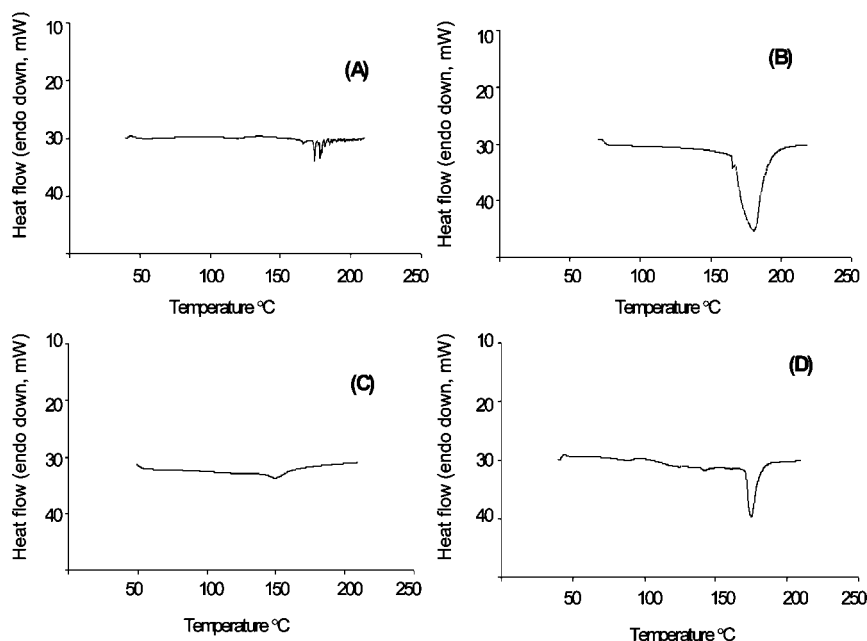


**Figure 2.** DSC thermograms of (A) of olive leaf extract, (B)  $\beta$ -CD, (C) inclusion complex of olive leaf extract/ $\beta$ -CD, and (D) physical mixture of olive leaf extract with  $\beta$ -CD.

low-energy interactions, such as hydrophobic interactions due to the displacement of water molecules from the cavity of the  $\beta$ -CD, increase of van der Waals interactions between the molecules, formation of hydrogen bonds, and other interactions. The change of entropy was also negative in this process. This behavior can be explained considering that the complexation caused a decrease in translational and rotational degrees of freedom of the complexed molecule as compared with the free one, resulting in a more ordered system. These results indicated that the complexation of olive leaf extract with  $\beta$ -CD has occurred. The Gibbs free energy change for the interactions that took place during the inclusion process may be calculated by the following equation:

$$\Delta G_{25} = \Delta H - T\Delta S \quad (3)$$

The Gibbs free energy at temperature 298 K was found as  $\Delta G_{25} = -14.3 \text{ kJ mol}^{-1}$  (Table 3), indicating that the inclusion process was spontaneous.

Figure 2 represents the DSC results of four different types of samples: olive leaf extract alone (Figure 2A),  $\beta$ -CD alone (Figure 2B), an inclusion complex (Figure 2C), and a physical mixture (Figure 2D). The DSC scan of olive leaf extract demonstrated an endothermic peak for this sample near 175 °C (the other peaks corresponded to other components present in the extract), which corresponded to the melting point of oleuropein. Similar results were obtained for the physical mixture of olive leaf extract and  $\beta$ -CD, presented in Figure 2D. The DSC thermogram of  $\beta$ -CD showed an endothermic peak at 175 °C (Figure 2B), possibly due to elimination of the contained water. The DSC scan of the physical mixture was almost identical to that of pure olive leaf extract and presented a strong endothermic peak, at the same temperature,  $\sim 175$  °C, showing that no inclusion in  $\beta$ -CD had occurred by this process. As can be seen in Figure 2B and Figure 2D, the thermograms of  $\beta$ -CD and of inclusion complex did not show any sharp endothermic peak in the temperature range investigated. The disappearance of the endothermic peak assigned to the constituents of the olive leaf extract at 175 °C (Figure 2C) indicated that the freeze-drying procedure produced an inclusion complex between olive leaf extract constituents and  $\beta$ -CD and not simply a physical mixture.

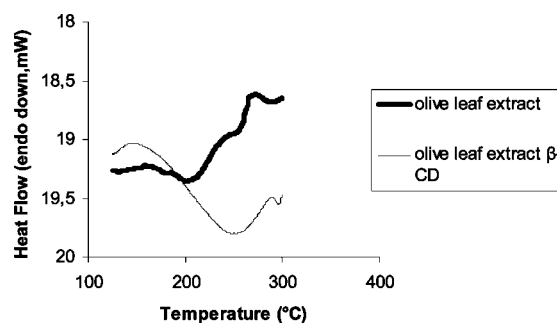


**Figure 3.** DSC thermograms of olive leaf extract and complex of olive leaf extract/ $\beta$ -CD under oxidative conditions.

In Figure 3 the DSC oxidation curves of olive leaf extract and of the inclusion complex of olive leaf extract with  $\beta$ -CD as a function of temperature and time are given. An exothermic peak was observed at 210 °C for oleuropein related to the oxidation or hydrolysis of oleuropein. The exothermic peak was not present in the DSC scan of the complex olive leaf extract/ $\beta$ -CD, which means that the olive leaf extract inside the cavity of  $\beta$ -CD was protected from oxidation.

The complexation of oleuropein with  $\beta$ -cyclodextrin has been previously studied by light scattering (22), and formation of a 1:1 complex was proposed. Complexation, however, involving inclusion is best documented using detailed NMR spectroscopic methods that allow observation of the cyclodextrin cavity interactions with specific parts of a guest molecule. Therefore, both pure oleuropein and the oleuropein-rich olive leaf extract have been utilized for the NMR study.

NMR spectroscopy has been used in the past to establish the structure of oleuropein (Figure 4) and other secoiridoids from *Olea europaea* or other plants (10, 33). The literature (10) describes the  $^1\text{H}$  and  $^{13}\text{C}$  NMR spectra in DMSO and methanol. Since the aqueous medium is necessary for complexation of oleuropein with  $\beta$ -CD, the NMR spectra of pure oleuropein were acquired in  $\text{D}_2\text{O}$ . The assignments (Figure 4) were based on 2D COSY and especially HSQC data (see Figure 1, Figure 2, and Table 1 of the Supporting Information) and are in agreement with those in the organic solvents mentioned above. The

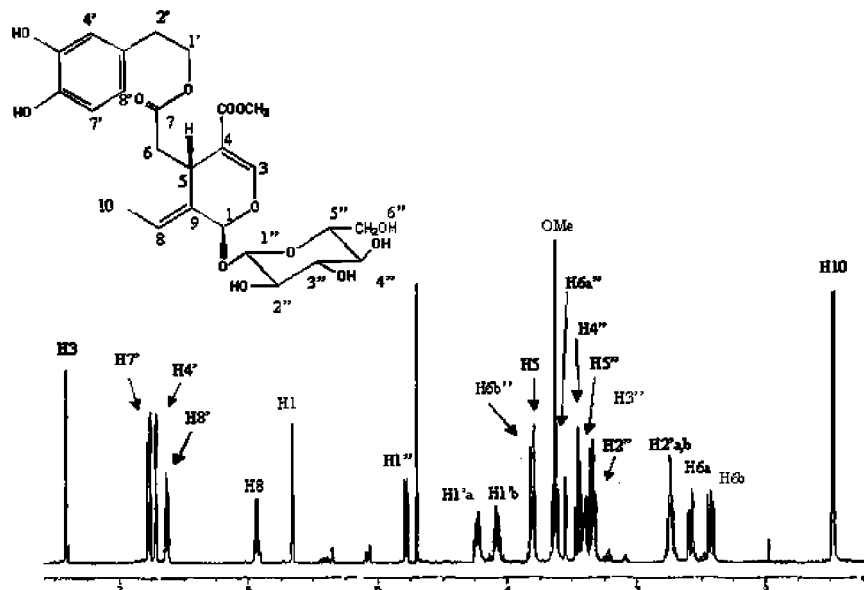


**Figure 4.** Structure of oleuropein with numbering and  $^1\text{H}$  NMR spectrum of oleuropein in  $\text{D}_2\text{O}$  acquired with presaturation of residual solvent peak (298 K). The presence of some impurities (<5%) does not inhibit the assignments.

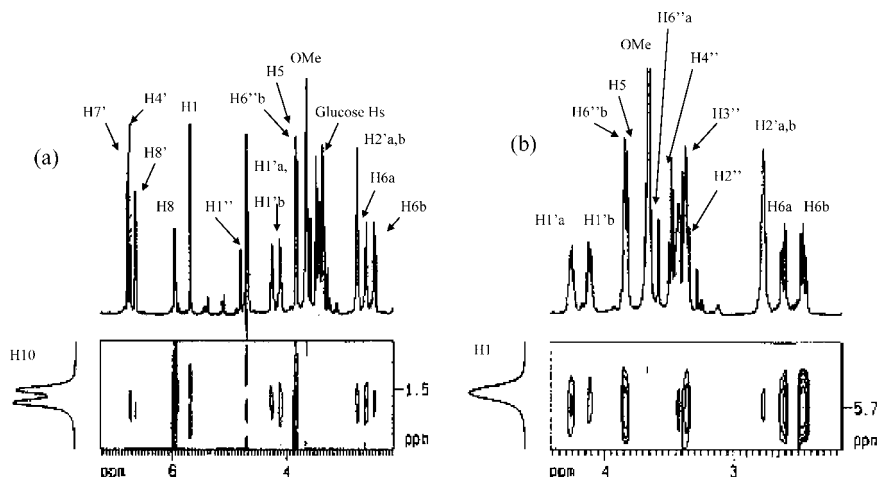


**Figure 5.** Parts of 2D ROESY map of pure oleuropein in  $\text{D}_2\text{O}$  at 300 K.

**Table 4.** Intramolecular Dipolar Interactions As Identified by NMR

Me10	H2'a,b, H4', H8', H1'a,b
H1	H1'', H1'a,b, H2'a,b

assignments were imperative since, in the presence of  $\beta\text{-CD}$ , the signals of the sugar part of oleuropein had to be singled out from those of  $\beta\text{-CD}$ . In order to investigate whether the aqueous environment has imposed particular conformation of oleuropein that could affect the mode of inclusion into  $\beta\text{-CD}$ , the 2D NOESY and ROESY spectra of oleuropein itself were also examined in  $\text{D}_2\text{O}$ . The NOE interactions detected were positive, as anticipated for this size of molecule, very weak, however, and few. On the contrary, the ROE interactions were numerous and easily observed (**Figure 5**). In order to avoid false conclusions arising from artifacts, known to appear in 2D ROESY spectra (mainly via TOCSY-type magnetization transfer), intramolecular ROE cross-peaks only between different spin coupling networks within the molecule were evaluated. **Table 4** shows the latter interactions, which indicate that in the aqueous environment the hydrophobic parts of the molecule, i.e., the phenethyl portion and the exocyclic allyl moiety, cradle together. The dihydroxyphenyl ring approaches the exocyclic methyl group and H1 of the hydroprane ring; therefore, considering a

3D model of oleuropein, a curling of the molecule takes place in  $\text{D}_2\text{O}$ . Such close contacts were not observed in 2D NOESY experiments of related secoiridoids lacking the sugar part, in organic solvents (9).

Addition of solid oleuropein into an aqueous solution of  $\beta\text{-CD}$  (either at 1:1 or at >1:1 mole ratio) caused large shielding in the cyclodextrin cavity protons (noted with bold H). Specifically, **H3** and **H5** were shielded by 27.8 and 63.2 Hz, respectively, indicating entrance of part of oleuropein molecule inside the cavity and formation of an inclusion complex (**Figure 6**).

In order to understand which part of oleuropein has been included in the  $\beta\text{-CD}$  cavity, the NMR spectra had to be assigned again in detail using 2D experiments since the region between 4.00 and 3.00 ppm is filled with many oleuropein and most of the CD protons (Figure 3 of the Supporting Information). It was found that the cavity protons **H3** and **H5** overlap with protons H5, H6''b and protons OMe, H6''a of oleuropein, respectively, whereas **H4** and **H2** completely obscure the sugar part of the guest, i.e., H4'', H5'', H3''. Primary **H6,6'** do not overlap with any oleuropein protons (Figure 4 of the Supporting Information). Comparison of the 2D ROESY maps (**Figure 7**) of the free guest (**Figure 7a**) and of the complex (**Figure 7b**) confirmed discrete differences, namely strong intermolecular

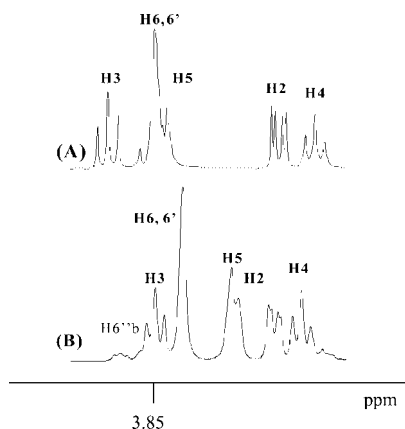


**Figure 6.** Partial  $^1\text{H}$  NMR spectra (500 MHz) of (A)  $\beta$ -CD alone and (B) in the presence of oleuropein in  $\text{D}_2\text{O}$ .

dipolar interactions of the three phenyl protons  $\text{H}4'$ ,  $\text{H}7'$ , and  $\text{H}8'$  with the cavity protons of  $\beta$ -CD  $\text{H}5$  and  $\text{H}3$  as well as  $\text{H}6,6'$ . Moreover, protons  $\text{H}1'$  and  $\text{H}2'$  of oleuropein interact with those of  $\beta$ -CD  $\text{H}3$  and  $\text{H}5$  and weakly with  $\text{H}6, \text{H}6'$  indicating deep inclusion involving the whole phenethyl part of the guest. The molecular orientation seems to be such that the primary side of  $\beta$ -CD is close to the aromatic OH, whereas the secondary side reaches down to  $\text{H}1'$ . The remaining ROE cross-peaks arose from intramolecular interactions; therefore, other parts of oleuropein are not included.

The formation of an inclusion complex between constituents of olive leaf extract (90.2% in oleuropein) was also examined in a similar manner (Figure 7c). Likewise, inclusion can be concluded for the aromatic part, as comparison of Figure 7c with Figure 7b showed mostly the same pattern. We thus propose that in the olive leaf extract/ $\beta$ -CD inclusion complex the aromatic ring of the main constituent, oleuropein, was included, as observed with the pure oleuropein. Since the extract was composed of other molecules with aromatic rings (e.g., hydroxytyrosol), these can also enter the cavity.

The NMR data have shown that in aqueous solution pure oleuropein forms a 1:1 complex with  $\beta$ -CD, inducing considerable shielding to the cavity protons, as the calculated binding constant of  $\sim 300 \text{ M}^{-1}$  would justify. The olive leaf extract behaves like pure oleuropein. Therefore, oxidation involving the dihydroxyphenyl ring can be minimized by inclusion, as shown by the DSC results. Examination of the olive leaf extract by NMR after standing for nearly 10 months in the aqueous solution showed some decomposition (new peaks had emerged), whereas the aqueous solution with  $\beta$ -CD after 5 months showed no new signals. Therefore, stability can be gained by inclusion, as shown by the DSC results.

## CONCLUSIONS

Phase solubility studies showed that encapsulation of olive leaf extract in  $\beta$ -cyclodextrin increased the aqueous solubility of the polyphenolic residue from olive leaf by more than 150%. Therefore, encapsulated olive leaf extract can be used as a food additive with the advantage of higher aqueous solubility. Moreover, oleuropein, which was the main constituent of olive leaf extract, is protected inside the cyclodextrin cavity from decomposition, as shown by the oxidative DSC studies. Therefore, the solid complex of olive leaf extract/ $\beta$ -CD can be used either to fortify foods or as a food supplement as the leaf extract alone with the advantage of increased stability.

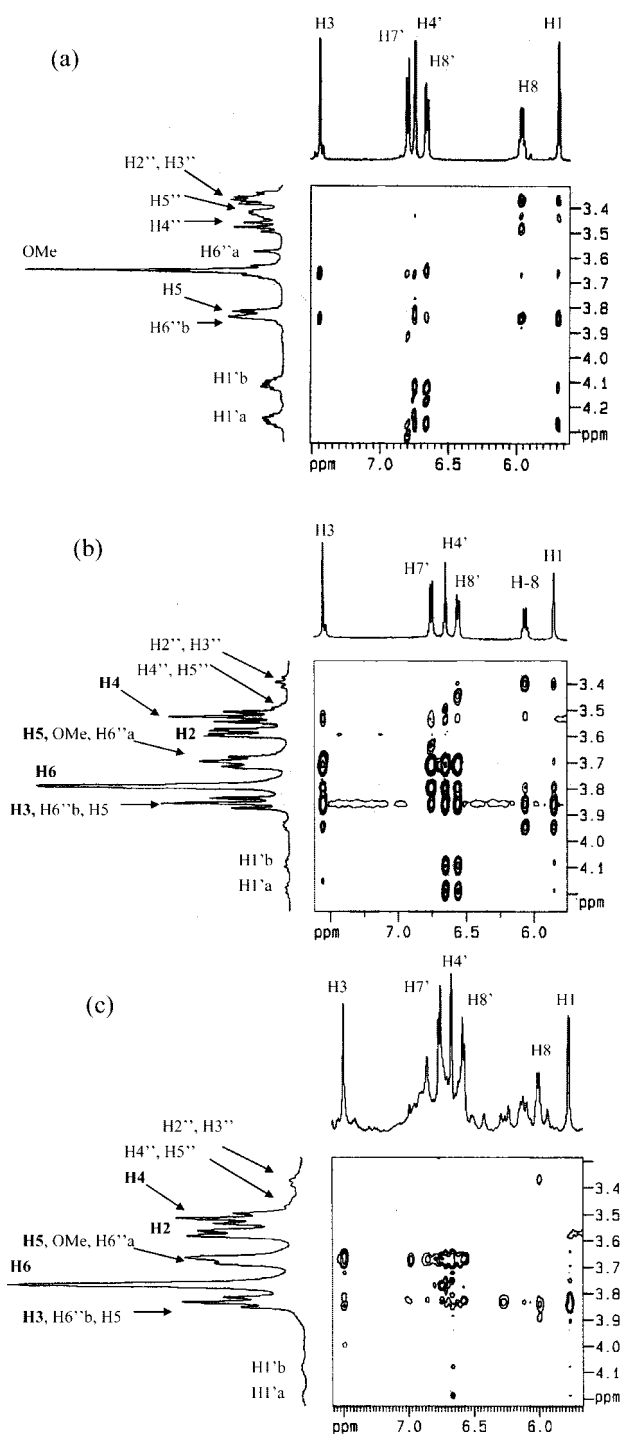


**Figure 7.** Part of the ROESY map of (a) oleuropein alone, (b)  $\beta$ -CD/oleuropein (1:1), and (c)  $\beta$ -CD/olive leaf extract (1:1) in  $\text{D}_2\text{O}$  at 300 K.

## ABBREVIATIONS USED

CD, cyclodextrin;  $\beta$ -CD, beta-cyclodextrin;  $K_c$ , stability constant;  $R$ , universal gas constant;  $\Delta H$ , enthalpy change;  $\Delta G_{25}$ , Gibbs free energy;  $T$ , absolute temperature;  $\Delta S$ , entropy change; NMR, nuclear magnetic resonance; DSC, differential scanning calorimetry.

**Supporting Information Available:** COSY and HSQC spectra of oleuropein and part of ROESY map of  $\beta$ -CD/oleuropein; table of NMR data of oleuropein. This material is available free of charge via the Internet at <http://pubs.acs.org>.

## LITERATURE CITED

- (1) Zeller, B. L.; Saleeb, F. Z.; Ludescher, R. D. Trends in development of porous carbohydrate food ingredients for use on flavor encapsulation. *Trends Food Sci. Technol.* **1999**, *9*, 389–394.
- (2) Gouin, S. Microencapsulation: Industrial appraisal of existing technologies and trends. *Trends Food Sci. Technol.* **2004**, *15*, 330–347.
- (3) Schrooyen, P. M. M.; van der Meer, R.; De Kruijff, C. G. Microencapsulation: its application in nutrition. *Proc. Nutr. Soc.* **2001**, *60*, 475–476.
- (4) Hedges, A. R.; Shieh, W. J.; Sikorski, C. T. Use of cyclodextrins for encapsulation in the use and treatment of food products. In Risch, S. J., Reineccius, G. A., Eds.; *Encapsulation and Controlled Release of Food Ingredients*; American Chemical Society: Washington, DC, 1995; Chapter 6, pp 60–71.
- (5) Szejtli, J. Introduction and general overview of cyclodextrin chemistry. *Chem. Rev.* **1998**, *98*, 1743–1753.
- (6) Polyakov, N. E.; Leshina, T.; Konovalova, T. A.; Hand, E. O.; Kispert, L. D. Inclusion complexes of carotenoids with cyclodextrins: NMR, EPR, and optical studies. *Free Radical Biol. Med.* **2004**, *36*, 872–880.
- (7) Szente, L.; Szejtli, J. Cyclodextrins as food ingredients. *Trends Food Sci. Technol.* **2004**, *15*, 137–142.
- (8) Somova, L. I.; Shode, F. O.; Ramnandan, P.; Nadar, A. Antihypertensive, antiatherosclerotic and antioxidant activity of triterpenoids isolated from *Olea europaea*, subspecies *africana* leaves. *J. Ethnopharmacol.* **2003**, *84*, 299–305.
- (9) Bouaziz, M.; Sayadi, S. Isolation and evaluation of antioxidants from leaves of a Tunisian cultivar olive tree. *Eur. J. Lipid Sci. Technol.* **2005**, *107*, 497–504.
- (10) Gariboldi, P.; Jommi, G.; Verotta, L. Secoiridoids from *Olea Europaea*. *Phytochemistry* **1986**, *25*, 865–896.
- (11) Soler-Rivas, C.; Espin, J. C.; Wichers, H. J. Oleuropein and related compounds. *J. Sci. Food Agric.* **2000**, *80*, 1013–1023.
- (12) Saenz, M. T.; Garcia, M. D.; Ahumada, M. C.; Ruiz, V. Cytostatic activity of some compounds from the unsaponifiable fraction obtained. *Il Farmaco* **1998**, *53*, 110–118.
- (13) Andrikopoulos, N. K.; Antonopoulou, S.; Kaliora, A. C. Oleuropein inhibits LDL oxidation induced by cooking oil frying by products and platelet aggregation induced by platelet-activating factor. *Lebensm. Wiss. Technol.* **2002**, *35*, 479–484.
- (14) Visioli, F.; Bellocchio, S.; Galli, C. Oleuropein, the bitter principles of olives, enhances nitric oxide production by mouse macrophages. *Life Sci.* **1998**, *62*, 541–546.
- (15) Miles, E. A.; Zoubouli, P.; Calder, P. C. Differential anti-inflammatory effects of phenolic compounds from extra virgin olive oil identified in human whole blood cultures. *Nutrition* **2005**, *21*, 389–394.
- (16) Furneri, P. M.; Marino, A.; Saija, A.; Uccella, N.; Bisignano, G. In vitro antimycoplasmal activity of oleuropein. *Int. J. Antimicrob. Agents* **2002**, *20*, 293–296.
- (17) Manna, C.; Migliardi, V.; Golino, P.; Scognamiglio, A.; Galletti, P.; Chiariello, M.; Zappia, V. Oleuropein prevents oxidative myocardial injury induced by ischemia and reperfusion. *J. Nutr. Biochem.* **2004**, *15*, 461–466.
- (18) Polzonetti, V.; Egidi, D.; Vita, A.; Vincenzetti, S.; Natalini, P. Involvement of oleuropein in (some) digestive metabolic pathways. *Food Chem.* **2004**, *88*, 11–15.
- (19) Andreadou, I.; Iliodromitis, E. K.; Mikros, E.; Constantinou, M.; Agalias, A.; Magiatis, P.; Skaltsounis, A. L.; Kamber, E.; Tsantili-Kakoulidou, A.; Kremastinos, D. T. The olive constituent oleuropein exhibits anti-ischemic, antioxidative, and hypolipidemic effects in anesthetized rabbits. *J. Nutr.* **2006**, *136*, 2213–2219.
- (20) Capasso, R.; Evidente, A.; Visca, C.; Gianfreda, L.; Maremonti, M.; Greco, G. Production of glucose and bioactive aglycone by chemical and enzymatic hydrolysis purified oleuropein from *Olea europaea*. *Appl. Biochem. Biotechnol.* **1996**, *60*, 365–377.
- (21) Mazzei, R.; Giorno, L.; Mazzuca, S.; Spadafora, A.; Drioli, E.  $\beta$ -Glucosidase separation from *Olea europaea* fruit and its use in membrane bioreactors for hydrolysis of oleuropein. *Desalination* **2006**, *200*, 483–484.
- (22) Briante, R.; La Cara, F.; Febbraio, F.; Patumi, M.; Nucci, R. Bioactive derivatives from oleuropein by a biotransformation on *Olea europaea* leaf extracts. *J. Biotechnol.* **2002**, *93*, 109–119.
- (23) Rodis, P. S.; Karathanos, V. T.; Mantzavinou, A. Partitioning of olive leaf antioxidants between oil and water phases. *J. Agric. Food Chem.* **2002**, *50*, 596–601.
- (24) Efmoropoulou, E.; Rodis, P. Complexation of oleuropein and trans-cinnamic acid with cyclodextrins. *Chem. Nat. Compd.* **2004**, *40*, 362–366.
- (25) Eliadou, K.; Yannakopoulou, K.; Rontoyianni, A.; Mavridis, I. M. NMR detection of simultaneous formation of [2]- and [3]pseudorotaxanes in aqueous solution between  $\alpha$ -cyclodextrin and linear aliphatic  $\alpha,\omega$ -aminoacids, an  $\alpha,\omega$ -diamine and an  $\alpha,\omega$ -diacid of similar length, and comparison with the solid state structures. *J. Org. Chem.* **1999**, *64*, 6217–6226.
- (26) Schneider, H. J.; Hacket, F.; Rudiger, V.; Ikeda, H. NMR studies of cyclodextrins and cyclodextrin complexes. *Chem. Rev.* **1998**, *98*, 1755–1785.
- (27) Williams, R. O.; Mahaguna, V.; Sriwongjanya, M. Characterization of an inclusion complex of cholesterol and hydroxypropyl- $\beta$ -cyclodextrin. *Eur. J. Pharm. Biopharm.* **1998**, *46*, 355–360.
- (28) Pralhad, T.; Rajendrakumar, K. Study of freeze-dried quercetin-cyclodextrin binary systems by DSC, FT-IR, X-ray diffraction and SEM analysis. *J. Pharm. Biomed.* **2004**, *34*, 333–339.
- (29) Rudnik, E.; Szczucinska, A.; Gwardiak, H.; Szulc, A.; Winiarska, A. Comparative studies of oxidative stability of linseed oil. *Thermochim. Acta* **2001**, *370*, 135–140.
- (30) Kalogeropoulos, N.; Chiou, A.; Mylona, A.; Ioannou, M. S.; Andrikopoulos, N. K. Recovery and distribution of natural antioxidants (a-tocopherol, polyphenols and terpenic acids) after pan-frying of Mediterranean finfish in virgin olive oil. *Food Chem.* **2007**, *100*, 509–517.
- (31) Higuchi, T.; Connors, K. A. Phase solubility technique. *Adv. Anal. Chem. Inst.* **1965**, *4*, 117–212.
- (32) Tommasini, S.; Raneri, D.; Ficarra, R.; Calabro, M. L.; Stancanelli, R.; Ficarra, P. Improvement in solubility and dissolution rate of flavonoids by complexation with  $\beta$ -cyclodextrin. *J. Pharm. Biomed.* **2004**, *35*, 379–387.
- (33) Calis, I.; Honsy, M.; Khalifa, T.; Nishibe, S. Secoiridoids from *Fraxinus angustifolia*. *Phytochemistry* **1993**, *33*, 1453–1456.

Received for review April 3, 2007. Revised manuscript received June 26, 2007. Accepted July 13, 2007.

JF0709698